Published in final edited form as:
*Magn Reson Med*. 2014 January ; 71(1): . doi:10.1002/mrm.24628.

# Whole-Heart Coronary MRA with 100% Respiratory Gating Efficiency: Self-Navigated Three-Dimensional Retrospective Image-Based Motion Correction (TRIM)

**Jianing Pang**[1,2], **Himanshu Bhat**[3], **Behzad Sharif**[2], **Zhaoyang Fan**[2], **Edward Gill**[2], **Louise E. J. Thomson**[2], **Troy LaBounty**[2], **John D. Friedman**[2], **Daniel S. Berman**[2], and **Debiao Li**[2,4]

[1]Northwestern University, Chicago, IL, USA

[2]Cedars-Sinai Medical Center, Los Angeles, CA, USA

[3]Siemens Medical Solutions USA Inc., Charlestown, MA, USA

[4]University of California, Los Angeles, CA, USA

## Abstract

**Purpose—**to develop a 3D retrospective image-based motion correction technique for whole-heart coronary MRA with self-navigation that eliminates both the need to setup a diaphragm navigator and gate the acquisition.

**Methods—**The proposed technique uses 1D self-navigation to track the superior-inferior (SI) translation of the heart, with which the acquired 3D radial k-space data is segmented into different respiratory bins. Respiratory motion is then estimated in image space using an affine transform model and subsequently this information is used to perform efficient motion correction in k-space. The performance of the proposed technique on healthy volunteers is compared with the conventional navigator gating approach as well as data binning using diaphragm navigator.

**Results—**The proposed method is able to reduce the imaging time to 7.1 ± 0.5 min from 13.9 ± 2.6 min with conventional navigator gating. The scan setup time is reduced as well due to the elimination of the navigator. The proposed method yields excellent image quality comparable to either conventional navigator gating or the navigator binning approach.

**Conclusion—**We have developed a new respiratory motion correction technique for coronary MRA that enables 1 $mm^3$ isotropic resolution and whole-heart coverage with 7 min of scan time. Further tests on patient population are needed to determine its clinical utility.

### Keywords

coronary MRA; respiratory motion correction; 3D affine transform; 3D radial acquisition

## Introduction

Free-breathing whole heart coronary MRA (CMRA) is a promising noninvasive method for diagnosing coronary artery disease. Currently, respiratory motion is detected by placing a pencil beam navigator on the dome of right hemi-diaphragm (RHD). The position of the lung-liver interface is then found using an edge detection algorithm. The segmented acquisition is typically gated using a fixed end-expiratory window, and a slice tracking

Correspondence to: Debiao Li, Ph.D., Biomedical Imaging Research Institute, Cedars-Sinai Medical Center, 8700 Beverly Blvd, PACT Suite 800, Los Angeles, CA, USA 90048, Phone: 310-423-7743; debiao.li@cshs.org.

approach is used with a correlation factor of 0.6 between diaphragm and heart motion to compensate for residual motion within the gating window [1, 2]. This navigator technique works rather well in practice, yet suffers from several shortcomings. Firstly, the diaphragm navigator needs multiple scout scans and time-consuming setup to ensure that the pencil beam is placed at the dome of RHD, the saturated slabs do not interfere with the region of interest (ROI), and the lung-liver interface is within the search region of the edge detection algorithm, which complicates workflow and requires specialized operator expertise. Secondly, due to the low efficiency of respiratory gating, imaging time can become quite long, which may cause patient discomfort, bulk movement, and drift in respiratory pattern and heart rate, all of which will potentially degrade the image quality. Moreover, the correlation between diaphragm and heart motions varies between subjects, thus using a fixed correlation factor can cause inaccurate estimation of heart motion [3, 4]. Lastly, only superior-inferior (SI) translation is accounted for. All other motion types, such as anterior-posterior (AP) and left-right (LR) translations, rotation, scaling, and shearing are neglected. It has been shown that, especially for larger acceptance windows, 3D translation or affine transform models are needed for accurate motion modeling [5].

Many works explored alternative methods to detect respiratory motion, including subject-specific heart-RHD correlation factors [6, 7], fat navigators [8–10], heart navigators [11], low resolution 2D images [12], as well as self-navigation, which was first pioneered by Larson et al for cardiac cine imaging [13], and subsequently used for coronary MRA with 1D [14–16] or 3D [17] motion detection capability. Another class of CMRA techniques has sought alternatives to the conventional gating approach in order to improve scan efficiency. For example, Moghari et al. proposed acquiring inner k-space lines with prospective navigator gating while gating the acquisition of the outer lines without reacquisition, and then using a compressed-sensing algorithm to reconstruct the undersampled k-space [18]. In another work by the same group, the size and position of the navigator gating window are adaptively determined for each subject to achieve a fixed scanning efficiency [19]. Several works were able to achieve 100% gating efficiency and used advanced motion models such as affine and non-rigid transform. Bhat et al. segmented 3D radial data into different respiratory bins for subsequent affine motion registration and correction [20].

Schmidt et al. interleaved 2D low-resolution slices with imaging lines to populate a 3D volume for non-rigid motion registration [21]. Both relied on the diaphragm navigator to resolve the respiratory state of the acquired k-space data. Alternatively, Stehning et al. and Piccini et al. proposed to detect and correct SI translational motion of the heart in a beat-by-beat fashion using SI self-navigation projections. To retrieve motion information, the former used the SI profile's center-of-mass, while the latter used a cross-correlation based method along with an automatic segmentation strategy for template selection [14, 16].

In this work, we report an improved respiratory motion correction scheme with self-navigation and image-based affine motion correction to achieve 100% scan efficiency. The general framework is adopted from Bhat et al [20]. However, 1D self-navigation is used in place of the diaphragm navigator to provide information on respiratory motion, enabling an easier and faster scan setup. The k-space data is then segmented into respiratory bins according to its respective respiratory position. The motion estimation between different bins is conducted in image space using an affine transform model, and the subsequent motion correction is performed efficiently by modifying the phase of k-space data and the shape of k-space trajectory. A final regridding concludes the reconstruction using the motion corrected data and trajectory. Performing motion correction, instead of gating the acquisition, reduces scan time and in turn improves robustness by reducing the chances of subject bulk motion. Healthy volunteer studies were conducted to evaluate the performance

of the proposed technique compared with both the conventional navigator gating and the navigator-based binning approach in [20].

## Methods

### Self-navigation

The pulse sequence is modified to include two additional readouts in the SI direction immediately before the imaging readouts (Fig. 1). With non-selective excitation associated with the 3D projection reconstruction (3DPR) trajectory, the Fourier transform of these lines represent the 1D Radon transforms (i.e. 1D projection) of the entire image volume. An AP dephasing gradient is added to the second readout to suppress chest wall signal [15]. Averaging of the two k-space lines creates a sinusoidal modulation of the underlying imaging volume. The following equation shows the calculation of the SI profile P(z) and describes the modulation effect from averaging:

$$P(z)=\frac{\int_{\mathrm{FOV}} c(\boldsymbol{r})\rho(\boldsymbol{r})\,dxdy+\int_{\mathrm{FOV}} c(\boldsymbol{r})\rho(\boldsymbol{r})e^{j\gamma G_{\mathrm{AP}} y\Delta t_{\mathrm{AP}}}\,dxdy}{2}=\int_{\mathrm{FOV}} c(\boldsymbol{r})\rho(\boldsymbol{r})\cos\left(\frac{1}{2}\gamma G_{\mathrm{AP}} y\Delta t_{\mathrm{AP}}\right) e^{j\gamma G_{\mathrm{AP}}\frac{y}{2}\Delta t_{\mathrm{AP}}}\,dxdy \quad [1]$$

where x, y and z are LR, AP and SI directions, respectively, ρ(x, y, z) and c(x, y, z) are magnetization distribution and coil sensitivity, respectively, γ is the gyromagnetic ratio, $G_{AP}$ and $\Delta t_{AP}$ are the amplitude and duration of the AP dephasing gradient, respectively. Combined with an appropriate choice of the AP dephasing gradient strength, the chest wall signal is effectively suppressed to improve motion detection (Eq. 1). In addition, only chest coils are used to minimize signal from the back, which is also static.

### Respiratory motion detection

The SI translation of the heart is detected from the acquired SI projection profile using a cross-correlation based method. The image space profile is interpolated eight fold to achieve sub-pixel resolution (~0.1 mm). The template is selected from a manually chosen end-expiratory line. The normalized cross-correlation between the template and every self-navigation profile is then calculated as follows:

$$C(u)=\frac{\sum_x\left[\left(f_u-\overline{f}_u\right)(T-\overline{T})\right]}{\sigma_f(u)\sigma_T} \quad [2]$$

where f is the self-navigation profile, T is the template, and u is the translation. $\bar{f}_u$ and $\sigma_f(u)$ are the average value and standard deviation of the profile within the template window, respectively, and $\bar{T}$ and $\sigma_T$ are the corresponding average and standard deviation for the template, respectively. The respiratory position d is then defined as the translation value (in pixels) which renders the largest normalized cross-correlation:

$$d=\mathrm{argmax}_{u\in}\quad C(u) \quad [3]$$

An example self-navigation profiles and the corresponding detected motion are shown in Fig. 2.

### Motion estimation and correction

The various degrees of freedom of respiratory motion in cardiac imaging are not limited to rigid translations. A 3D affine transform, characterized by a linear transform of the coordinates and 3D translations, is a more realistic model for respiratory motion as it

includes translation, rotation, scaling, and shearing. Therefore, it is used in this work for motion estimation. Taking into account the static features in the imaged FOV such as chest wall and spine, the motion estimation is performed after applying a 3D mask containing only the heart region. The motion estimation program is written in C using the Insight Toolkit (ITK), an open-source image processing toolkit [22]. Rather than prospectively rejecting any portion of the acquired data, all of the k-space lines are segmented into six respiratory bins according to the corresponding respiratory positions hence achieving 100% scan efficiency. From each bin a low-resolution 3D image is reconstructed. Since the k-space pattern in each bin is generally non-uniform and undersampled, straightforward regridding using the analytical $1/k_r^2$ density compensation will show a considerable amount of streaking artifacts. To suppress these artifacts, a low-pass filter is computed adaptively based on the Nyquist radius of the undersampled k-space and is then applied to the k-space data before regridding. One of the six bins is identified as end-expiratory and the corresponding low-resolution image is set as the reference. The other five bins are then registered to the reference using the masked affine model, resulting in an affine matrix and a translation vector for each bin, which will be stored for subsequent motion correction, as described next.

It is well known that translations in image space correspond to linear phase modulations in k-space. In fact, a general affine transform of image space coordinates corresponds to an affine transform of k-space coordinates [23]. Therefore, knowing the image-space transform parameters, motion correction can be directly conducted in k-space, without the need to grid the k-space data and perform time-consuming image space interpolation as in [20]. The following equation describes the relation between the acquired and affine-motion-corrected datasets:

$$F'_n(\boldsymbol{k}) = \frac{\exp\left(j2\pi(A_n^{-T}\boldsymbol{k}^{\boldsymbol{T}}\boldsymbol{b_n})\right)}{|\det(A_n)|} F_n(A_n^{-T}\boldsymbol{k_n}) \quad [4]$$

where $F_n(\boldsymbol{k})$ and $F'_n(\boldsymbol{k})$ are the acquired and corrected k-space for bin n, respectively, and $A_n$ and $\boldsymbol{b}_n$ are the corresponding affine matrix and translation vector, respectively. The new k-space data and trajectory are fed into a regular regridding program to reconstruct the final motion corrected image. Compared with the image-domain registration method in [20] using ITK, this approach is significantly faster (<1 min vs. 25 min, for a four channel dataset). Fig. 3 summarizes the workflow of the proposed method.

## In vivo experiments

In vivo experiments were performed on clinical 1.5 T scanners (MAGNETOM Espree and Avanto, Siemens AG Healthcare, Erlangen, Germany) with institutional review board approval and written consent obtained before each exam. A 12-channel cardiac coil was used for data acquisition. Whole-heart coronary MRA images were acquired using an ECG-gated, T2-prepared, fat-saturated bSSFP sequence with a 3D radial trajectory [24]. The sequence was modified to include self-navigation readouts, while the diaphragm navigator module was kept for comparison purposes. The scan parameters were as follows: TR/TE = 3.2 ms/1.6 ms, FOV = $260^3$ – $300^3$ $mm^3$, matrix size = $256^3$, voxel size = 1.0 – 1.2 $mm^3$ interpolated to 0.5 – 0.6 $mm^3$, 250 μs hard pulse with flip angle = 90°, readout bandwidth = 781 Hz/pixel, 15 preparation pulses in each heartbeat with linear flip angle modulation [25], T2-prep duration = 40 ms, chemically selective fat-saturation, 25 – 40 lines per heartbeat in data acquisition windows of 80 – 130 ms, 16000 to 16800 total projections. A four chamber cine scan was performed to determine the quiescent imaging window.

In order to compare the proposed method with conventional navigator gating, a first group of five healthy volunteers (average age 26.7±3.0 years, 1 woman, 4 men) were scanned with

the above sequence and the acquisition was gated by respiratory navigator. From the raw dataset, a motion-free and a motion corrupted dataset were extracted as shown in Fig. 5. In the gated acquisition, each k-space segment was repeatedly acquired until the navigator position falls into the acceptance window. Therefore, the gated data was obtained by extracting the last repetition of each segment, and extracting the first repetitions generated a free-breathing, motion-corrupted data. This approach minimizes confounding factors such as patient movement and heart-rate variation between scans. Three 3D images were reconstructed for each subject: one from the prospectively gated data (Gated), one from the motion corrupted data without any correction (NC), and one with the proposed motion correction technique applied to the motion corrupted data (TRIM).

To further determine the performance of the proposed self-navigated technique, a second group of 12 healthy volunteers (average age 33±7.6 years, 3 women, 9 men) were scanned. Specifically, the new technique was compared with the previous navigator-based binning method that uses the same pulse sequence. Both diaphragm navigator and self-navigation data were collected but the acquisition was not gated. By this means, self-navigation was compared with diaphragm navigator as a data binning method, with the same k-space sampling strategy [20]. Three 3D images were reconstructed from a raw dataset: without correction (NC), corrected with navigator binning (NAV-bin), and one with the proposed technique (TRIM).

Image reconstruction is done off-line using MATLAB (Mathworks, Natick, MA) with parallel computing toolbox on a Dell Precision T7500 workstation. All images were reformatted using CoronaViz software (Siemens Corporate Research, Princeton, NJ). Quantitative measurement of LAD, LCX and RCA length and sharpness were performed automatically using the same software. Qualitative image scoring was also performed by two independent and experienced readers that were blinded to different techniques on a five point scale (0–4): 0, no coronary arteries are visible, 1, coronary arteries are visible but of non-diagnostic quality; 2, coronary arteries are of diagnostic quality but very blurred; 3, coronary arteries are of diagnostic quality and slightly blurred; 4, excellent image quality with minimal to no blurring.

## Results

For the comparison between NC, Gated and TRIM, both Gated and TRIM showed better ($P$<0.05) image qualities than NC in terms of qualitative scores and LAD, LCX and RCA length and sharpness. No significant differences were found between Gated and TRIM in both qualitative and quantitative evaluations. Notably, imaging time with TRIM (7.1 ± 0.5 min) was significantly shorter than that using Gated (13.9 ± 2.6 min) due to 100% gating efficiency ($P$<0.05). Results are summarized in Fig. 5.

Fig. 6 shows a coronal slice as an example comparison between NC, Gated and TRIM. Without any motion correction, the image is blurry and has poor visualization of the example RCA segment. The navigator gated image shows good image quality at a cost of a significantly longer scan time. With imaging time same as the ungated one, the proposed method significantly reduces motion blurring and yield excellent coronary artery visualization.

For the comparison between NC, NAV-bin and TRIM, both NAV-bin and TRIM had better ($P$<0.05) image qualities than NC in terms of qualitative scores and LAD, LCX and RCA length and sharpness. In addition, no significant differences in image qualities were found between NAV-bin and TRIM. The scan time is 7.6 ± 1.5 min for all three methods. Results are summarized in Fig. 7.

Fig. 8 shows reformatted coronary artery images from five healthy subjects comparing NC, NAV-bin and TRIM. Without any motion correction (first column), the images are blurry and have poor visualization of the coronary arteries. With imaging time unchanged and without the need to set up a navigator, the proposed motion correction technique (second column) significantly reduces motion blurring and shows excellent coronary artery visualization. The navigator binning approach (third column) shows similar improvements.

## Discussion

We have presented in this work a retrospective image-based respiratory motion correction method with self-navigation for whole-heart coronary MRA. The self-navigation signal is used to segment k-space data into different respiratory bins, facilitating affine motion estimation of the moving bins with respect to a selected reference bin. The motion correction is conducted very efficiently by modifying k-space phase and trajectory, and the final image is reconstructed by regridding the motion-corrected data.

The proposed method provides a number of advantages compared with previous works. Firstly, prescribing the diaphragm navigator requires additional time to perform multiple scout scans in order to position the crossed pair of slices onto RHD. The time-consuming procedure complicates the setup process of CMRA protocols and requires specialized operator expertise. Therefore, compared with techniques that require navigators [6–11, 18–21], using self-navigation will save a significant amount of scanner time and make whole-heart CMRA protocols much more user friendly. Secondly, the scan duration with navigator gating is usually significantly prolonged and unpredictable, due to the fact that the scan efficiency (ratio between accepted and total acquired data) is usually low (around 40%) and highly dependent on the subject's breathing pattern. In addition, especially low navigator efficiency usually indicates an unsuccessful scan [26, 27]. By accepting all free-breathing data and performing retrospective binning and image-based motion correction, the proposed method is able to make the scan time both shorter and less variable, which reduces subject discomfort, and in turn the chances of bulk motion and respiratory pattern drift, thus improving the robustness of CMRA. Thirdly, the proposed method performs motion correction using an affine transform, which better characterizes the respiratory motion than translation-only models [6, 7, 14–17]. This is especially necessary for larger acceptance windows [5]. Lastly, it has been shown that there can be a hysteresis between diaphragm and heart motion, resulting in inaccurate motion detection with the diaphragm navigator [28]. Although not shown in this study, self-navigation can avoid this potential error by directly tracking heart position. On healthy volunteers, the proposed method was able to provide excellent coronary artery delineation and 1 mm isotropic spatial resolution with a scan time of around 7 min, or 500 heartbeats. In the future, it needs to be further tested on CAD patients in order to evaluate its performance in visualizing coronary stenoses of various degrees and at different locations.

The proposed method has several limitations, upon which future improvements can be made. Firstly, Bhat et al concluded by simulation that approximately 40 heart beats are needed in each bin in order to guarantee an accurate motion estimation [20]. This is often violated for subjects with irregular breathing patterns. For example, as shown in Fig. 9, outlier respiratory positions will result in some bins having too few projections to reconstruct an adequate image for motion estimation. Currently, if a first binning results in one or more bins with insufficient number of projections, the data corresponding to the outliers (defined as more than two standard deviations away from the median) are discarded, and the remaining data is reprocessed. Secondly, for subjects with very deep breathing, using a fixed number of bins may result in a good amount of residual intra-bin motion. Alternatively, the number of bins, as well as the size and position of each individual bin may

be adaptively determined to better segment k-space data; hence, trading between the accuracy of motion estimation, which corresponds to the amount of data in one bin, and residual motion, which corresponds to bin size.

Moreover, it is shown that for some subjects there is a hysteresis between RHD and heart position, therefore a particular diaphragm position may correspond to two different heart positions and shapes for inspiration/expiration [28]. The proposed method uses self-navigation to avoid this ambiguity but still assumes a one-to-one relationship between the SI heart translation and other motion parameters, such as AP and LR translation. It has been shown that hysteresis can be present in between SI/AP or SI/LR translations [17], which could be a potential source of residual motion artifacts in some subjects and needs further investigation.

Lastly, the most time-consuming step in the current reconstruction scheme is the 3D affine motion estimation with the ITK software package. The overall processing time of the proposed method (~1 hour) significantly limits its clinical feasibility, even though we have employed parallel computing to achieve multi-fold acceleration (by processing different channels and bins simultaneously). The motion estimation program uses a gradient descent algorithm that converges slowly especially when the motion is significant, e.g., for bins far away from the reference bin. It is possible to detect bulk translation parameters, in a beat-by-beat fashion, from self-navigation projections in one or more directions. Correcting for translations first will accelerate the iterative motion estimation process as the bins to be registered are now “closer” to the reference. This may also help in resolving some of the intra-bin translational motion.

## Conclusions

In conclusion, we have developed a respiratory motion correction method for whole-heart coronary MRA combining self-navigation and image-based motion correction to achieve 100% gating efficiency, eliminating both the need of setting up a diaphragm navigator and gating the acquisition, hence provides a smooth workflow and enables high isotropic resolution (1 $mm^3$) and whole heart coverage in a short scan time (7 min). Excellent image quality was achieved in healthy volunteers. The clinical utility of the proposed method needs to be tested on patients.

## Acknowledgments

This project was supported in part by NIH grant numbers HL38698 and EB002623.

## References

1. Danias PG, McConnell MV, Khasgiwala VC, Chuang ML, Edelman RR, Manning WJ. Prospective navigator correction of image position for coronary MR angiography. Radiology. 1997; 203:733–736. [PubMed: 9169696]
2. Wang Y, Riederer SJ, Ehman RL. Respiratory motion of the heart: kinematics and the implications for the spatial resolution in coronary imaging. Magn Reson Med. 1995; 33:713–719. [PubMed: 7596276]
3. Wang Y, Ehman RL. Retrospective adaptive motion correction for navigator-gated 3D coronary MR angiography. J Magn Reson Imaging. 2000; 11:208–214. [PubMed: 10713956]
4. Nagel E, Bornstedt A, Schnackenburg B, Hug J, Oswald H, Fleck E. Optimization of real time adaptive navigator correction for 3D magnetic resonance coronary angiography. Magn Reson Med. 1999; 42:408–411. [PubMed: 10440967]

5. Manke D, Nehrke K, Bornert P, Rosch P, Dossel O. Respiratory motion in coronary magnetic resonance angiography: a comparison of different motion models. J Magn Reson Imaging. 2002; 15:661–671. [PubMed: 12112516]
6. Taylor AM, Keegan J, Jhooti P, Firmin DN, Pennell DJ. Calculation of a subject-specific adaptive motion-correction factor for improved real-time navigator echo-gated magnetic resonance coronary angiography. J Cardiovasc Magn Reson. 1999; 1:131–138. [PubMed: 11550345]
7. Moghari MH, Hu P, Kissinger KV, Goddu B, Goepfert L, Ngo L, Manning WJ, Nezafat R. Subject-specific estimation of respiratory navigator tracking factor for free-breathing cardiovascular MR. Magn Reson Med. 2012; 67:1665–1672. [PubMed: 22134885]
8. Keegan J, Gatehouse PD, Yang GZ, Firmin DN. Non-model-based correction of respiratory motion using beat-to-beat 3D spiral fat-selective imaging. J Magn Reson Imaging. 2007; 26:624–629. [PubMed: 17729350]
9. Nguyen TD, Nuval A, Mulukutla S, Wang Y. Direct monitoring of coronary artery motion with cardiac fat navigator echoes. Magn Reson Med. 2003; 50:235–241. [PubMed: 12876698]
10. Nguyen TD, Spincemaille P, Prince MR, Wang Y. Cardiac fat navigator-gated steady-state free precession 3D magnetic resonance angiography of coronary arteries. Magn Reson Med. 2006; 56:210–215. [PubMed: 16767743]
11. Manke D, Nehrke K, Bornert P. Novel prospective respiratory motion correction approach for free-breathing coronary MR angiography using a patient-adapted affine motion model. Magn Reson Med. 2003; 50:122–131. [PubMed: 12815687]
12. Henningsson M, Koken P, Stehning C, Razavi R, Prieto C, Botnar RM. Whole-heart coronary MR angiography with 2D self-navigated image reconstruction. Magn Reson Med. 2012; 67:437–445. [PubMed: 21656563]
13. Larson AC, White RD, Laub G, McVeigh ER, Li D, Simonetti OP. Self-gated cardiac cine MRI. Magn Reson Med. 2004; 51:93–102. [PubMed: 14705049]
14. Stehning C, Bornert P, Nehrke K, Eggers H, Stuber M. Free-breathing whole-heart coronary MRA with 3D radial SSFP and self-navigated image reconstruction. Magn Reson Med. 2005; 54:476–480. [PubMed: 16032682]
15. Lai P, Larson AC, Bi X, Jerecic R, Li D. A dual-projection respiratory self-gating technique for whole-heart coronary MRA. J Magn Reson Imaging. 2008; 28:612–620. [PubMed: 18777542]
16. Piccini D, Littmann A, Nielles-Vallespin S, Zenge MO. Respiratory self-navigation for whole-heart bright-blood coronary MRI: methods for robust isolation and automatic segmentation of the blood pool. Magn Reson Med. 2012; 68:571–579. [PubMed: 22213169]
17. Lai P, Bi X, Jerecic R, Li D. A respiratory self-gating technique with 3D-translation compensation for free-breathing whole-heart coronary MRA. Magn Reson Med. 2009; 62:731–738. [PubMed: 19526514]
18. Moghari MH, Akcakaya M, O'Connor A, Basha TA, Casanova M, Stanton D, Goepfert L, Kissinger KV, Goddu B, Chuang ML, Tarokh V, Manning WJ, Nezafat R. Compressed-sensing motion compensation (CosMo): a joint prospective-retrospective respiratory navigator for coronary MRI. Magn Reson Med. 2011; 66:1674–1681. [PubMed: 21671266]
19. Moghari MH, Chan RH, Hong SN, Shaw JL, Goepfert LA, Kissinger KV, Goddu B, Josephson ME, Manning WJ, Nezafat R. Free-breathing cardiac MR with a fixed navigator efficiency using adaptive gating window size. Magn Reson Med. 201210.1002/mrm.24210
20. Bhat H, Ge L, Nielles-Vallespin S, Zuehlsdorff S, Li D. 3D radial sampling and 3D affine transform-based respiratory motion correction technique for free-breathing whole-heart coronary MRA with 100% imaging efficiency. Magn Reson Med. 2011; 65:1269–1277. [PubMed: 21500255]
21. Schmidt JF, Buehrer M, Boesiger P, Kozerke S. Nonrigid retrospective respiratory motion correction in whole-heart coronary MRA. Magn Reson Med. 2011; 66:1541–1549. [PubMed: 21604297]
22. Luis, I.; Schroeder, W.; Ng, L.; Cates, J. The ITK Software Guide. 22005. (www.itk.org) at ISCUpdated for ITK version 2.4
23. Shechter G, McVeigh ER. MR Motion Correction of 3D Affine Deformations. Proceedings Int Soc Mag Reson Med. 2003

24. Stehning C, Bornert P, Nehrke K, Eggers H, Dossel O. Fast isotropic volumetric coronary MR angiography using free-breathing 3D radial balanced FFE acquisition. Magn Reson Med. 2004; 52:197–203. [PubMed: 15236387]

25. Deshpande VS, Chung YC, Zhang Q, Shea SM, Li D. Reduction of transient signal oscillations in true-FISP using a linear flip angle series magnetization preparation. Magn Reson Med. 2003; 49:151–157. [PubMed: 12509831]

26. Sakuma H, Ichikawa Y, Chino S, Hirano T, Makino K, Takeda K. Detection of coronary artery stenosis with whole-heart coronary magnetic resonance angiography. J Am Coll Cardiol. 2006; 48:1946–1950. [PubMed: 17112982]

27. Kato S, Kitagawa K, Ishida N, Ishida M, Nagata M, Ichikawa Y, Katahira K, Matsumoto Y, Seo K, Ochiai R, Kobayashi Y, Sakuma H. Assessment of coronary artery disease using magnetic resonance coronary angiography: a national multicenter trial. J Am Coll Cardiol. 2010; 56:983–991. [PubMed: 20828652]

28. Nehrke K, Bornert P, Manke D, Bock JC. Free-breathing cardiac MR imaging: study of implications of respiratory motion--initial results. Radiology. 2001; 220:810–815. [PubMed: 11526286]

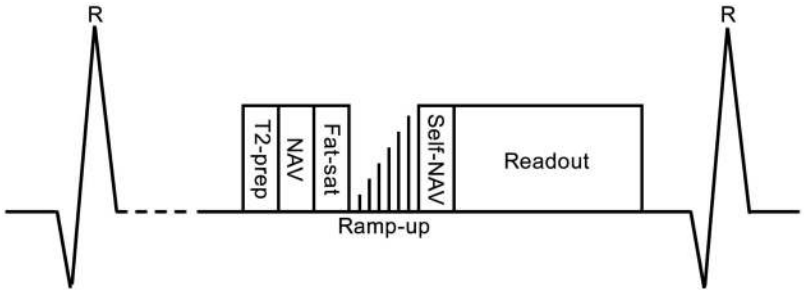


**Figure 1.**
Schematic of the pulse sequence showing the acquisition scheme for one heartbeat. The ECG gated, free-breathing scan acquires the data during a total of ~500 heartbeats.

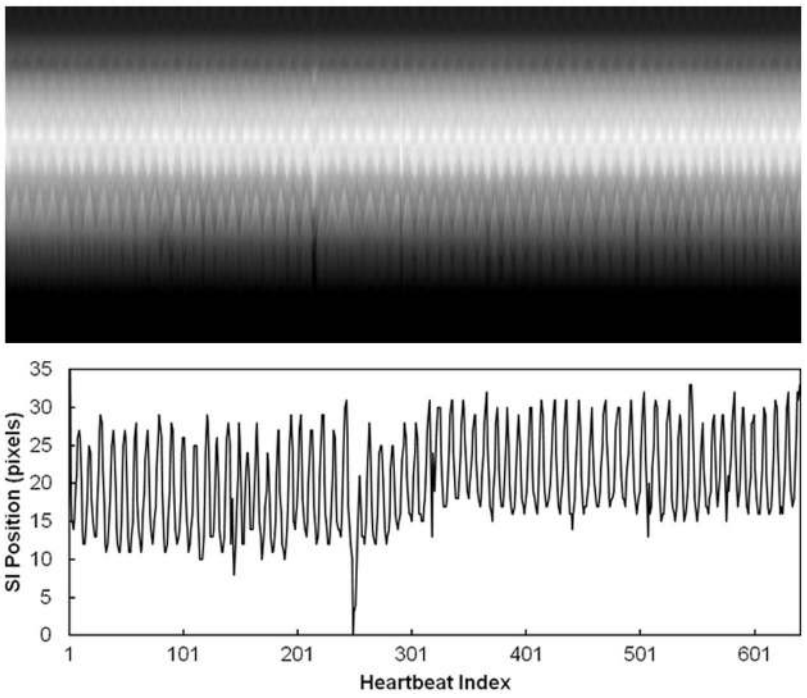


**Figure 2.**
Top: time series of the self-navigation profiles. Bottom: detected SI motion of the heart

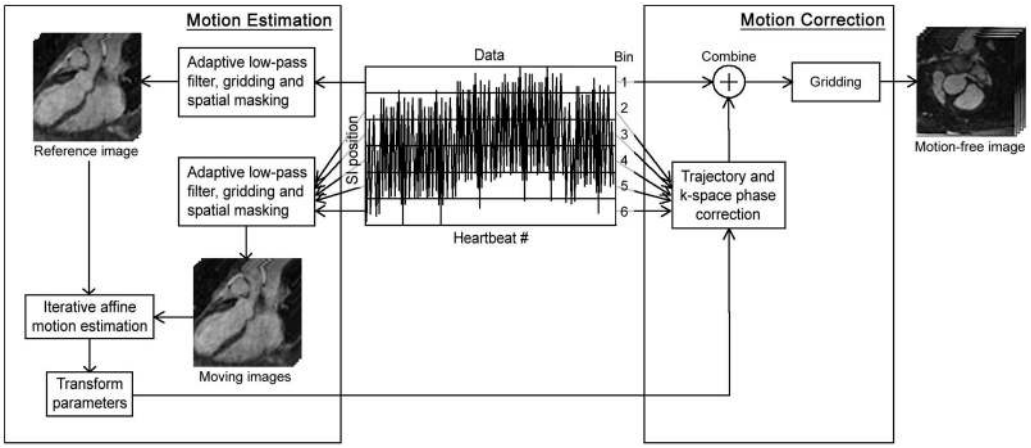


**Figure 3.**

Workflow of TRIM: K-space data is first segmented into different respiratory bins, and then from each bin a low resolution image representing different respiratory stage is reconstructed. With one bin as reference the affine motion parameters of all other bins are calculated and stored for the k-space motion correction. Finally all data is regridded with the corrected trajectory and phase to yield a motion-free image.

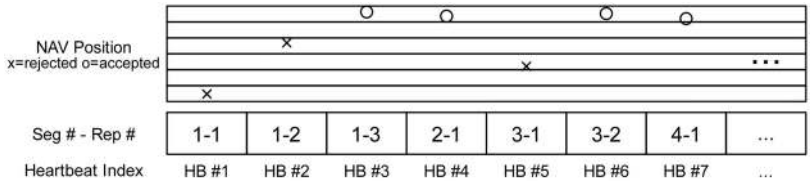


**Figure 4.**

Schematics of data extraction. In this example, for the motion-free dataset the extracted blocks will be 1-3, 2-1, 3-2, 4-1… and for the motion-corrupted dataset the blocks will be 1-1, 2-1, 3-1, 4-1…

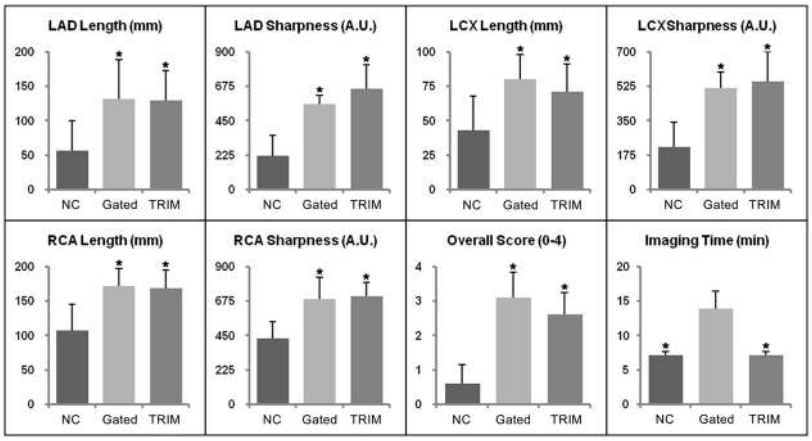


**Figure 5.**
Comparisons of the performance of NC, Gated and TRIM. (*P<0.05)

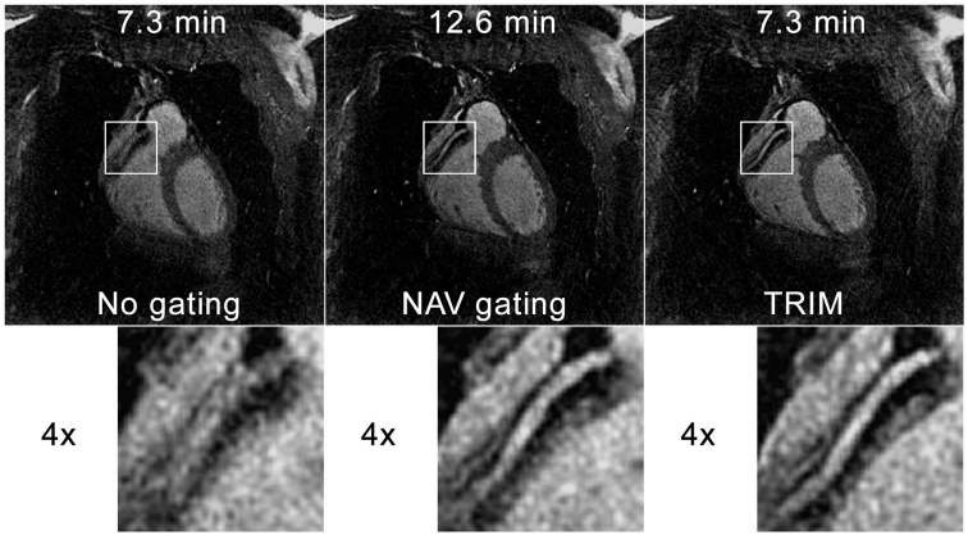


**Figure 6.**
Comparison of ungated and uncorrected image (left), image with conventional navigator gating (middle) and with the proposed motion correction method (right). As can be seen the proposed method delivers excellent image quality without the penalty in scan time.

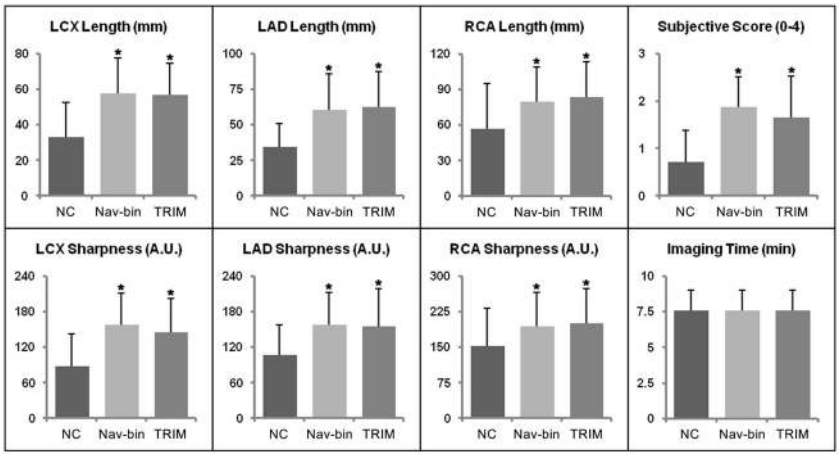


**Figure 7.**
Comparisons of the performance of NC, NAV-bin and TRIM. (*P<0.05)

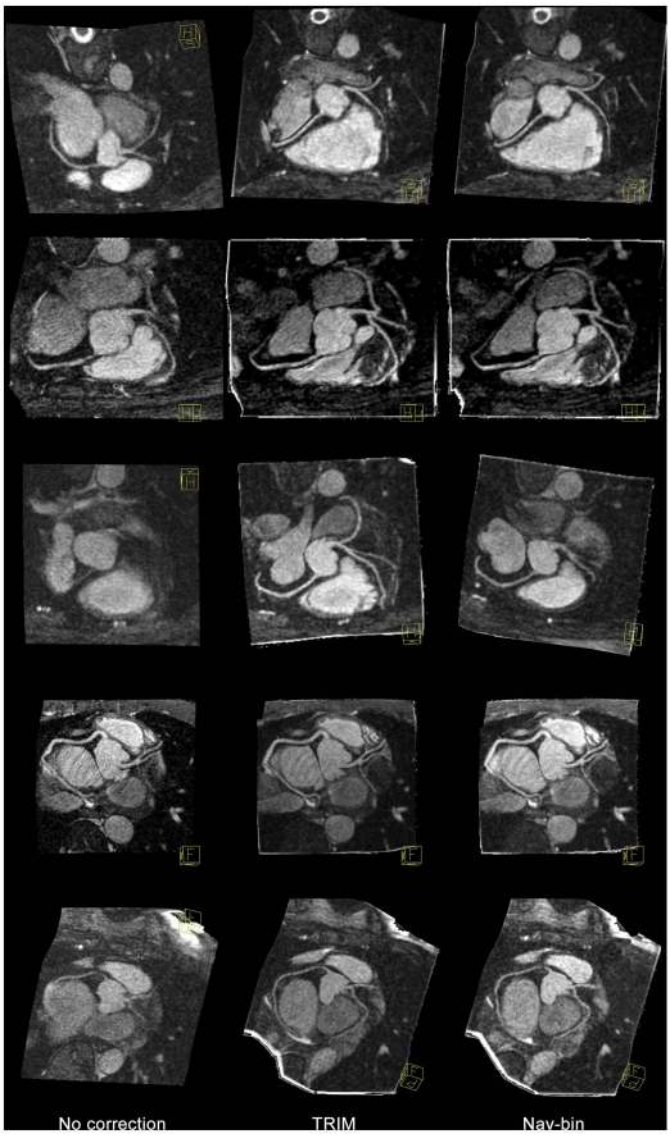


**Figure 8.**
Comparison of the reformatted images: no correction (left), NAV-bin (middle), TRIM (right). As can be seen TRIM delivers excellent image quality without the need for a diaphragm navigator.

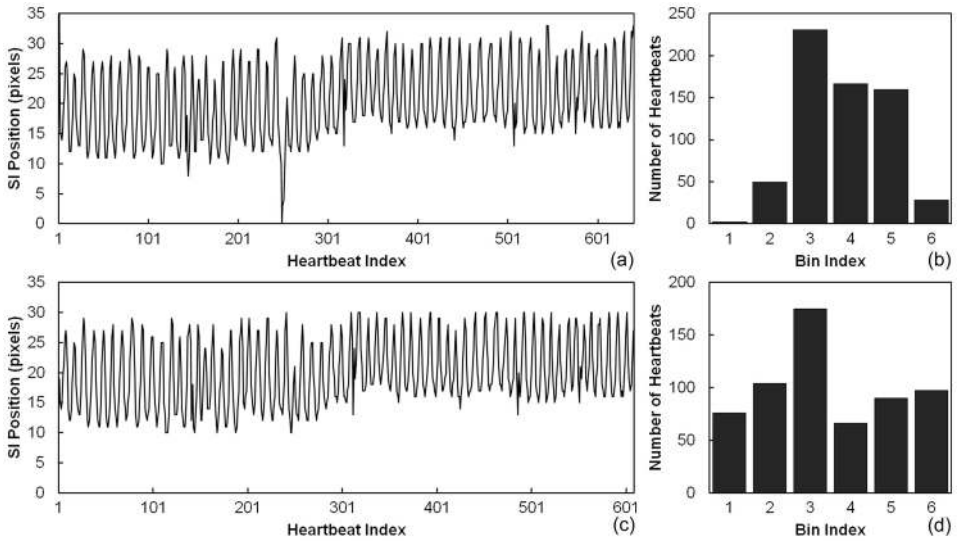


**Figure 9.**

Effect of outlier respiratory positions on binning. In this example, the original respiratory pattern (a) has outlier positions around the 250th heartbeat. The corresponding binning result (b) has bin 1 and bin 6 with insufficient number of heartbeats. The processed respiratory pattern (c) with the outliers discarded results in a more uniform binning result (d) that allows subsequent accurate motion estimation.